Article

Flotillin and RacH modulate the intracellular immunity of Dictyostelium to Mycobacterium marinum infection

HAGEDORN, Monica, SOLDATI, Thierry

Abstract

Mycobacterium marinum, a close relative of Mycobacterium tuberculosis, provides a useful model to study the pathogenesis of tuberculosis in genetically tractable model organisms. Using the amoeba Dictyostelium discoideum as a host, we show that expression of the M. marinum protein MAG24-1 is crucial to interfere with phagosome maturation. We find that two host proteins - the flotillin homologue vacuolin and p80, a predicted copper transporter - accumulate at the vacuole during pathogen replication until it finally ruptures and the bacteria are released into the host cytosol. Flotillin-1 accumulation at the replication niche and its rupture were also observed in human peripheral blood monocytes. By infecting various Dictyostelium mutants, we show that the absence of one of the two Dictyostelium vacuolin isoforms renders the host more immune to M. marinum. Conversely, the absence of the small GTPase RacH renders the host more susceptible to M. marinum proliferation but inhibits its cell-to-cell spreading.

Reference

HAGEDORN, Monica, SOLDATI, Thierry. Flotillin and RacH modulate the intracellular immunity of Dictyostelium to Mycobacterium marinum infection. *Cellular microbiology*, 2007, vol. 9, no. 11, p. 2716-33

DOI : 10.1111/j.1462-5822.2007.00993.x
PMID : 17587329

Cellular Microbiology (2007) **9**(11), 2716–2733
doi:10.1111/j.1462-5822.2007.00993.x
First published online 24 June 2007

Flotillin and RacH modulate the intracellular immunity of *Dictyostelium* to *Mycobacterium marinum* infection

Monica Hagedorn and Thierry Soldati*
Département de Biochimie, Faculté des Sciences, Université de Genève, Sciences II, 30 quai Ernest Ansermet, CH-1211-Genève-4, Switzerland.

Summary

***Mycobacterium marinum*, a close relative of *Mycobacterium tuberculosis*, provides a useful model to study the pathogenesis of tuberculosis in genetically tractable model organisms. Using the amoeba *Dictyostelium discoideum* as a host, we show that expression of the *M. marinum* protein MAG24-1 is crucial to interfere with phagosome maturation. We find that two host proteins – the flotillin homologue vacuolin and p80, a predicted copper transporter – accumulate at the vacuole during pathogen replication until it finally ruptures and the bacteria are released into the host cytosol. Flotillin-1 accumulation at the replication niche and its rupture were also observed in human peripheral blood monocytes. By infecting various *Dictyostelium* mutants, we show that the absence of one of the two *Dictyostelium* vacuolin isoforms renders the host more immune to *M. marinum*. Conversely, the absence of the small GTPase RacH renders the host more susceptible to *M. marinum* proliferation but inhibits its cell-to-cell spreading.**

Introduction

Pathogenic mycobacteria – including the causative agent of tuberculosis, *Mycobacterium tuberculosis* – pose a major threat to public health. They proliferate within macrophages and other 'professional' phagocytes of the immune system whose mission is to kill bacterial invaders. Upon their phagocytosis, pathogenic mycobacteria prevent the remodelling of the phagosome into a bactericidal phagolysosome, so converting the compartment into a custom-built 'niche' for proliferation (Vergne *et al*., 2004a). During phagocytosis of inert particles and non-infectious bacteria, the vacuolar H^+-ATPase is delivered early to the phagosomes causing lumenal acidification. Lysosomal glycoproteins, such as Lamp-1 (Aniento *et al*., 1993), are delivered to the acidifying phagosomes, which also accumulate the membrane raft protein flotillin-1 (Dermine *et al*., 2001) and lipids such as lysobisphosphatidic acid (LBPA; Kobayashi *et al*., 1998). Soon after their phagocytosis, pathogenic mycobacteria are able to change the course of phagosome maturation, resulting in only limited acidification that correlates with a paucity of the vacuolar H^+-ATPase (Sturgill-Koszycki *et al*., 1994). Mycobacteria also limit the accumulation of lysosomal hydrolases (Vergne *et al*., 2004a); however, the compartment in which they proliferate remains fusogenic, dynamic and partly connected to the host endocytic pathway (Sturgill-Koszycki *et al*., 1996). To our knowledge, no marker has been identified that accumulates specifically in or around this niche, except the actin-binding protein coronin. But a functional role for coronin in mycobacteria infection is disputed. Whereas active recruitment of coronin to the *M. tuberculosis* replication vacuole has been reported to stimulate intravacuolar proliferation in a murine macrophage cell line (Ferrari *et al*., 1999), in human macrophages association of coronin was not necessary for maintenance of the *M. tuberculosis* proliferation niche (Schuller *et al*., 2001). Targeted disruption of the orthologous coronin gene in *Dictyostelium* even slightly increased susceptibility to *M. marinum* infection (Solomon *et al*., 2003). The ultimate fate of the mycobacteria replication vacuole and the mechanisms of release and dissemination of the pathogen remain largely unknown.

Mycobacterium marinum, a close relative of *M. tuberculosis*, is a pathogen of fish and amphibians that causes systemic tuberculosis-like diseases in its natural hosts (Swaim *et al*., 2006). The course of infection, granuloma formation and structure are indistinguishable from the infection and lesions caused by *M. tuberculosis* (Swaim *et al*., 2006), and their intracellular proliferation niches are very similar (Barker *et al*., 1997). Several *M. marinum* virulence mutants have similar phenotypes to *M. tuberculosis* mutants and can be complemented by *M. tuberculosis* genes (Gao *et al*., 2003a,b; 2004; 2006; Volkman *et al*., 2004; Cosma *et al*., 2006; Tan *et al*., 2006). Thus, it has become a useful model to study the pathogenesis of tuberculosis in genetically tractable model organisms such as zebrafish (Pozos and Ramakrishnan, 2004) and *Drosophila* (Dionne *et al*., 2003). The molecular processes by which mycobacteria

Received 30 March, 2007; revised 29 May, 2007; accepted 30 May, 2007. *For correspondence. E-mail thierry.soldati@biochem.unige.ch; Tel. (+41) 22 379 6496; Fax (+41) 22 379 6399.

manipulate their host cells and spread from cell to cell are topics of intense research. Recently, extended RD1 (regions of difference 1) gene clusters, which are missing from non-tuberculous mycobacteria and are thought to be important in immunopathology, were found to encode factors which are essential for virulence of *M. tuberculosis* and *M. marinum* (Gao *et al*., 2004; Cosma *et al*., 2006; Tan *et al*., 2006). Members of two large related mycobacterial multigene families, PE (Pro–Glu motifs) and PPE (Pro–Pro–Glu motifs), were shown to be associated with duplication of the RD1 gene clusters (van Pittius *et al*., 2006). Previous genetic screenings and transposon mutagenesis studies suggested that this protein superfamily might contain virulence and antigenicity factors, but very little is known about their precise functions, times and places of action. In *M. marinum*, two orthologues of the PE-PGRS (polymorphic GC-repetitive sequence) subfamily of PE proteins, MAG24-1 and MAG24-3 (Ramakrishnan *et al*., 2000), are required for efficient replication of *M. marinum* in mammalian macrophages and in leopard frogs and *Drosophila* (Ramakrishnan *et al*., 2000; Dionne *et al*., 2003). Strains carrying transposon insertions into these two loci (*M. marinum* L1D and L2D respectively) are avirulent in leopard frogs and *Drosophila* (Ramakrishnan *et al*., 2000; Dionne *et al*., 2003). The macrophage-activated promoter map24 controls expression of MAG24-1 during infection of these hosts (Ramakrishnan *et al*., 2000; Dionne *et al*., 2003). The strong correlation between switching on the map24 promoter and successful infection makes map24 activation a simple marker of infection and a useful analytical tool to pinpoint activation of the proliferation programme.

It has been widely accepted that *M. tuberculosis* proliferates principally, if not exclusively, inside its replication vacuole, and the infection is thought to spread when the cells lyse (Gao *et al*., 2004). In contrast, *M. marinum* has been seen outside its vacuole, moving around the cytoplasm of mouse and fish macrophages powered by a polymerizing actin 'comet tail', a process suggested to play a role in the dissemination of infection (Stamm *et al*., 2003; 2005). Whether *M. marinum* further replicates in the cytosol remains debated. Very recent evidence might reconcile these two opposing views, as escape from the vacuole has now been reported for *M. tuberculosis* and *M. leprae* in myeloid cells (van der Wel *et al*., 2007).

Dictyostelium is a useful model to study conserved host–pathogen interactions with *Pseudomonas* (Cosson *et al*. 2002, Pukatzki *et al*., 2002), *Legionella* (Solomon *et al*., 2000; Hagele *et al*., 2000; Weber *et al*. 2006) and *Vibrio cholera* (Pukatzki *et al*., 2006). Two recent studies have revealed the potential of *Dictyostelium* as a model host in which to study mycobacteria infections (Solomon *et al*., 2003; Peracino *et al*., 2006). This social amoeba is a professional phagocyte that lives in the soil and feeds on bacteria. Phagocytosis and phagosomal maturation in *Dictyostelium* are well understood at the molecular and proteomic levels and are very similar to the processes in mammals (Gotthardt *et al*., 2002; 2006; Maniak, 2002; Neuhaus *et al*., 2002). After the usual phases of acidification and digestion of the particle, vacuolins, like mammalian flotillin, are recruited to phagosomes during the late stage of maturation (Jenne *et al*., 1998; Gotthardt *et al*., 2006). During this late phase, the reneutralized compartment prepares to exocytose its undigested contents (Rauchenberger *et al*., 1997). Vacuolins were recently recognized as flotillin family proteins (Wienke *et al*., 2006). The *Dictyostelium* genome encodes three highly homologous isoforms of vacuolin, two of which, vacuolins A and B, are expressed in vegetative cells. Cells lacking vacuolin A have no obvious mutant phenotype, but absence of vacuolin B affects the organization and morphology of the endocytic pathway and prolongs the endosomal transit time for fluid and particles, with a concomitant prolongation of the acidic phase of maturation (Jenne *et al*., 1998). The morphology and function of the vacuolin-positive late endosomes are controlled in part by a Rac GTPase, RacH (Somesh *et al*., 2006). As in cells lacking vacuolin B, absence of RacH prolongs the endosomal transit time but, contrary to what is observed in *vacB*$^-$ cells, endolysosomal acidification is drastically reduced, and phagosomal acidification absent (Somesh *et al*., 2006).

Here, we have studied the phagocytosis of *M. marinum* by *Dictyostelium*, its manipulation of the phagocytic vacuole to bypass maturation, and subsequent replication of the bacteria inside this niche. We find that two host proteins, vacuolin B and p80, accumulate at the *M. marinum* replication vacuole. Functional studies with *Dictyostelium* mutants demonstrated that vacuolin B and the RacH GTPase are important players in the establishment and/or the maintenance of this replication niche. In addition, we found that RacH is essential for cell-to-cell spreading of the mycobacteria infection.

Results

Characterization of an infection cycle

Two recent studies reported that pathogenic mycobacteria proliferate in *Dictyostelium* over the course of a 4- to 7-day incubation (Solomon *et al*., 2003; Peracino *et al*., 2006). To identify host modulators that play a role in mycobacterial infection, we dissected the early phase of this infection process in more detail. Monolayers of adherent *Dictyostelium* cells were infected by centrifuging mycobacteria onto them; this ensured efficient and synchronous phagocytosis of the bacteria and, by varying the multiplicity of infection (moi), enabled us to control the

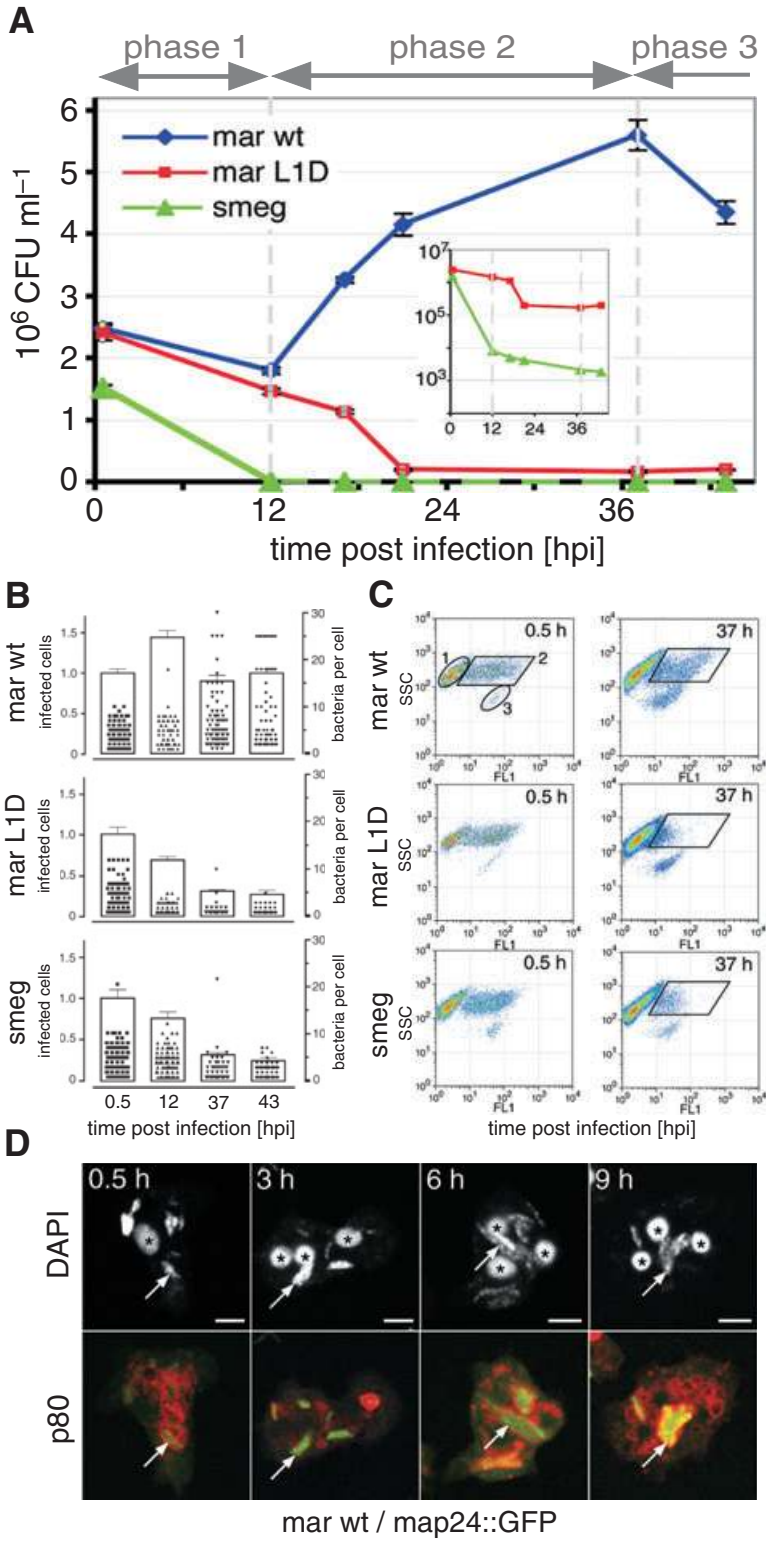

Fig. 1. Characterization of an initial cycle of infection, proliferation and release. Adherent *Dictyostelium* cells were infected with GFP-expressing wild-type *M. marinum* (mar wt), avirulent *M. marinum* L1D (mar L1D) and non-pathogenic *M. smegmatis* (smeg) by centrifuging the mycobacteria onto the cells. After removal of uningested mycobacteria, the cells were incubated for 0–43 h.
A. At the indicated times, the number of live bacteria was determined by counting cfu. In cells infected with *M. marinum* L1D or *M. smegmatis*, the number of live bacteria decreased steadily but with different kinetics (see inset for comparison on a logarithmic scale plot). Three phases of infection could be discerned in cells infected with wild-type *M. marinum*: an initial lag phase (phase 1), followed by a burst of proliferation (phase 2) and finally a plateau or small decrease (phase 3). Points and error bars indicate mean ± SEM of triplicate experiments.
B. The proportion of infected cells (bar graph ± SEM) and the number of bacteria per cell (dot plot) were scored for each bacteria strain by direct visualization using a fluorescence microscope
C. In FACS analysis, plotting side-scattering (SSC) as a function of fluorescence (FL1) revealed three populations: non-infected cells (1), cells harbouring fluorescent mycobacteria (2) and fluorescent extracellular mycobacteria (3). At 0.5 h post infection (hpi), the proportion of cells with fluorescent mycobacteria was very similar for all three strains, but the evolution with time was markedly different. Whereas the population of cells containing *M. marinum* L1D and *M. smegmatis* decreased and were almost absent at 37 h, the population of cells infected with *M. marinum* persisted and increased in total fluorescence.
D. *Dictyostelium* cells were infected with *M. marinum* carrying the map24::GFP vector. At the indicated times, cells were stained for the p80 marker (red, bottom) and DNA was visualized with DAPI (top). Mycobacteria (arrows) showed accumulation of GFP (green, bottom) as early as 3 hpi, and the intensity of GFP fluorescence continued to rise until 9 hpi. Asterisks indicate DAPI-stained *Dictyostelium* nuclei (top). Scale bars, 5 μm.

proportion of cells that engulfed a bacterium. Contrary to what has been reported (Solomon *et al*., 2003; Peracino *et al*., 2006), we did not observe cytotoxicity even at moi as high as 100. We monitored bacterial proliferation inside the host cells with three independent techniques (Fig. 1A–C). First, the number of live bacteria in the infected culture was determined by counting colony-forming units (cfu; Fig. 1A). Second, the proportion of

infected cells and the number of GFP-expressing bacteria in host cells was quantified using immunofluorescence microscopy (Fig. 1B). Finally, the population dynamics of cells infected with fluorescent bacteria were analysed by fluorescence-activated cell sorting (FACS; Fig. 1C).

Dictyostelium provided an efficient host for *M. marinum* (mar wt) proliferation. The profile of changes in cfu during the first 2 days post infection revealed three distinct phases: an initial lag phase lasting 12 h post infection (hpi, Fig. 1A, phase 1); a major proliferation phase 12–37 hpi, in which the number of cfu increased two- to sixfold (phase 2), followed by a plateau or decrease in the number of cfu after 37 hpi (phase 3). We define this three-phase profile as a unit cycle of infection. In contrast, the non-pathogenic strain *Mycobacterium smegmatis* (smeg) and the avirulent *M. marinum* mutant strain L1D (mar L1D) failed to proliferate (Fig. 1A). The number of cfu of *M. smegmatis* fell at least 100-fold within the first 12 hpi (Fig. 1A, inset), followed by a steady but slower decrease. The number of *M. marinum* L1D cfu decreased more slowly (10- to 100-fold within 43 hpi), possibly reflecting a balance between a low level of proliferation and inefficient killing (Fig. 1A).

We confirmed and quantified these findings by fluorescence microscopy (Fig. 1B). The number of GFP-expressing *M. marinum* increased from an average of 3.3 at 0.5 hpi to an average of 9 and a maximum of 25 per cell at 37 hpi (Fig. 1B, dot plot). The number of infected cells remained relatively constant (Fig. 1B, bar graph); the transient increase in the proportion of infected cells 12 hpi may be due to phagocytosis of bacteria that adhered to the cell surface even after washing at time zero. The small decrease in the proportion of infected cells at 37 hpi may result from loss of fluorescence due to the death of intracellular bacteria, from the release of bacteria from the cells or from the death of infected cells. The proportion of cells infected with *M. smegmatis* and *M. marinum* L1D decreased by 70–80% over the course of the incubation period (Fig. 1B, bar graph), concomitant with a decrease in the number of bacteria per infected cell (Fig. 1B, dot plot). As already indicated by the cfu analyses, however, there were significant quantitative differences between these two strains: the average number of bacteria per cell at 12 hpi was 4.15 for *M. smegmatis*, but only 1.73 for *M. marinum* L1D (Fig. 1B, dot plot).

FACS was used to obtain a quantitative readout of population changes during infection. By plotting side-scatter (SSC) versus green fluorescence (FL1), three populations were distinguished: uninfected cells (Fig. 1C, population 1), host cells infected with GFP-expressing bacteria (population 2), and extracellular bacteria (population 3). For all three strains, at 0.5 hpi, very few extracellular bacteria were present and 28–30% of cells had ingested green fluorescent bacteria. The population of cells infected with *M. marinum* persisted up to 37 hpi. During phase 2, an overall increase in the fluorescent signal from both intra- and extracellular bacteria indicated intracellular growth of GFP-expressing bacteria and their partial release into the extracellular milieu. In contrast, the populations of cells infected with *M. smegmatis* and *M. marinum* L1D both declined significantly and to similar levels after 37 hpi (Fig. 1C).

Our data indicate that the lag phase (phase 1) reflects the early and active manipulation of *Dictyostelium* by *M. marinum* to convert phagosomes into replication niches. Consistent with this interpretation, expression of GFP driven by the map24 promoter was detectable as early as 3 hpi and continued to increase up to 9 hpi, a sign that the pathogen has switched on its infection programme (Fig. 1D).

To precisely determine the fate of mycobacteria during the initial steps of an infection, we examined the colocalization of fluorescent bacteria with well-defined maturation markers (Fig. 2) (Sturgill-Koszycki *et al*., 1996; Ravanel *et al*., 2001; Gotthardt *et al*., 2002; 2006). In *Dictyostelium*, phagosome maturation takes place within 90 min after uptake. In accordance with the normal sequence of events, during that period, phagosomes containing *M. smegmatis* and *M. marinum* L1D received the vacuolar H^+-ATPase [up to 76% and 91% positive at 20 min post infection (mpi) respectively], the endosomal marker p80 (up to 93 and 86% positive at 90 mpi respectively) and, as they progress through late stages, vacuolin (up to 36% and 45% positive at 90 mpi respectively) (Fig. 2A). In addition, *M. marinum* L1D was exocytosed within 1–3 hpi (Fig. S1). Interestingly, the vacuolar H^+-ATPase was also transiently present in 60% of the phagosomes containing *M. marinum*. To illustrate the transience of the delivery of VatA to the mycobacteria phagosomes, illustrative examples of immunofluorescence stainings are shown for all strains at 20 mpi and 90 mpi (Fig. 2B). Further progression of phagosomes containing *M. marinum* through the maturation programme was profoundly altered. Indeed, the number of p80-positive *M. marinum* phagosomes increased more slowly up to only 36% at 90 mpi and vacuolin was detected only on 7% of the phagosomes at that time (Fig. 2A). This situation persisted during the remaining of phase 1, as illustrated for the 6 hpi time point in Fig. S2. After the 90 mpi time point, all the phagosomes containing *M. smegmatis* and *M. marinum* L1D continued to be positive for one or a combination of the maturation markers (data shown for 6 hpi in Fig. S2). In sharp contrast, after the transient recruitment observed at 90 mpi, the signal for VatA in phagosomes containing wild-type *M. marinum* decreased to undetectable levels, and was not replaced by the recruitment of later markers. Indeed, during phase 1 less than 8% of these vacuoles were ever positive for vacuolin or cathepsin D (data shown for 6 hpi in Fig. S2).

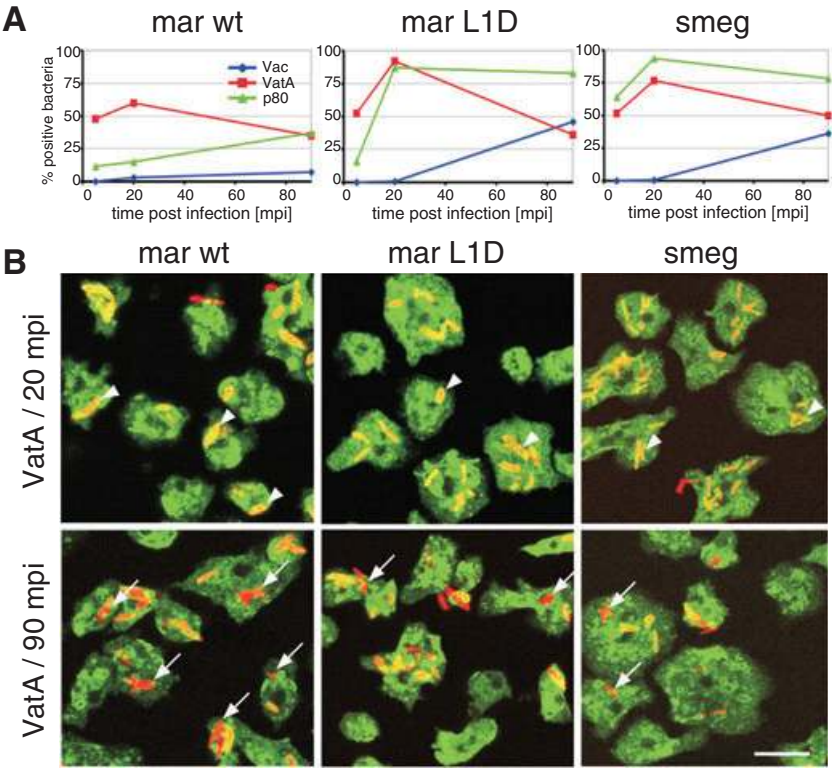

Fig. 2. *Mycobacterium marinum* interferes with the normal phagosome maturation process. During the first 90 min post infection (mpi), the fate of all three strains, wild-type *M. marinum*, *M. marinum* L1D and *M. smegmatis*, was monitored by immunofluorescent colocalization with well-characterized maturation markers: a subunit of the vacuolar H^+-ATPase (VatA), the endosomal membrane protein p80 and the flotillin homologue, vacuolin (Vac). Note that the anti-vacuolin antibody does not distinguish between the vacuolin isoforms.
A. Bacteria colocalizing with each of the markers were scored at the indicated times.
B. Representative images of colocalization with the VatA subunit at 20 mpi and 90 mpi are shown for all three strains. At 20 mpi bacteria were observed in compartments which were strongly labelled with VatA (white arrowheads). Towards the end of the normal phagosomal maturation programme (90 mpi), VatA was partially retrieved from these phagosomes and bacteria were observed with weak or no colocalization (indicated by white arrows). Scale bar, 5 μm.

From the transient presence of VatA in phagosomes containing *M. marinum* and the quasi-absence of later maturation markers, we conclude that this pathogen arrests or bypasses phagosome maturation and replicates efficiently in *Dictyostelium* as it does in other host systems (Ramakrishnan *et al.*, 2000; Dionne *et al.*, 2003). In addition, the protein MAG24-1 that is not expressed in *M. marinum* L1D is essential early in phase 1 to ensure successful infection.

Vacuolin, the Dictyostelium *flotillin, accumulates at the replication niche during phase 2*

We examined the genesis of the replication niche during phase 2 of infection by performing immunofluorescence microscopy on cells infected with the three mycobacteria strains. As expected, at 12 hpi, most compartments containing *M. smegmatis* (smeg) or *M. marinum* L1D (mar L1D) were positive for vacuolin and/or cathepsin D, indicative of late digestive phagosomes prepared for exocytosis (Fig. 3A and 12 hpi). The situation did not change during phase 2: both the non-pathogenic and the avirulent bacteria were observed mainly in tightly apposed membrane-bound compartments containing cathepsin D and surrounded by vacuolin (Fig. 3A and 37 hpi). The patchy vacuolin staining pattern resembled that reported for post-lysosomes (Jenne *et al.*, 1998). Surprisingly, even though the vacuole containing *M. marinum* did not follow the normal course of maturation during phase 1, the post-lysosomal marker vacuolin was detectable around the bacteria at 12 hpi (Fig. 3A and 12 hpi), and, up to 37 hpi, the vacuolin staining surrounding distended vacuoles increased to extremely high levels (Fig. 3A and 37 hpi).

This gradual and strong accumulation of vacuolin during phase 2 allowed us to follow the morphological changes to the replication niche that accompany bacteria proliferation (Fig. 3B). The membrane of the vacuole was initially tightly apposed to the bacteria but as they proliferated it became distended and apparently spacious (Fig. 3B; we designate this as 'stage 1' in the development of the replication niche); the size of the vacuole increased and its membrane appeared to be pushed from inside by the growing rods of bacteria, producing sharp deformations of the vacuolar membrane (Fig. 3B; stage 2). At later times (21–37 hpi), distortion of the vacuole was eventually followed by its rupture and release of the bacteria into the cytosol (Fig. 3B; stage 3). Bacteria were frequently observed associated with remnants of their ruptured compartments, as well as in the cytosol of cells with completely disorganized vacuolin-positive compartments (Fig. 3B; stage 4). We also detected strong accumulation of p80 at the replication niche. Based on extensive sequence homology with copper transporters from many organisms (Nose *et al.*, 2006), this membrane protein is predicted to be a copper transporter and is ubiquitous throughout the endocytic and phagocytic pathways

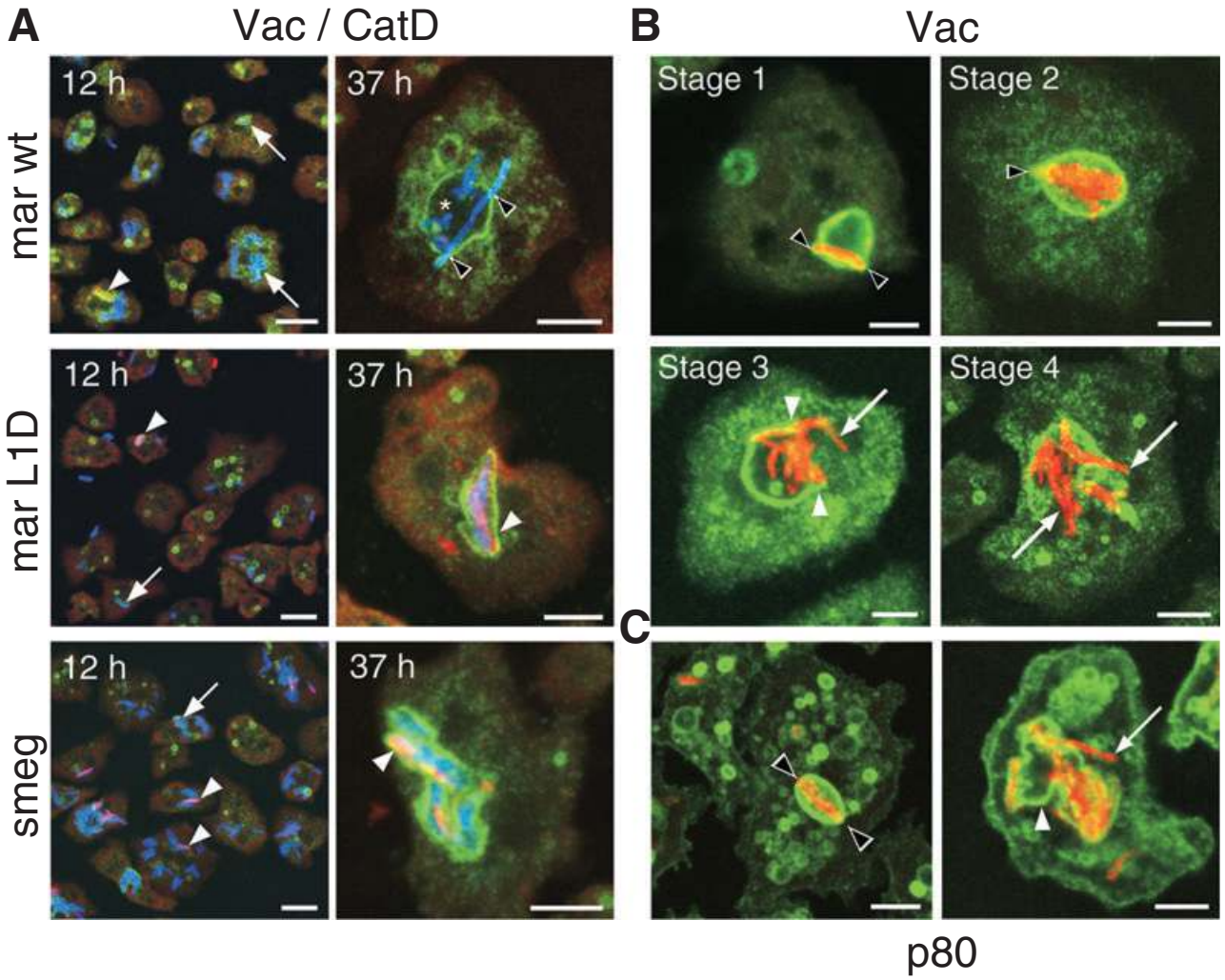

Fig. 3. Establishment and rupture of the proliferation niche of *M. marinum* in *Dictyostelium*. Uptake of the three fluorescent mycobacteria strains [blue in (A) and red in (B) and (C)] was performed as in Fig. 1 and their fate monitored at the boundary between phases 1 and 2 of infection by immunofluorescent staining of cathepsin D (CatD, red) and vacuolin (Vac, green).
A. At 12 hpi, a large proportion of *M. marinum* L1D and *M. smegmatis* were positive for one or both markers (arrowheads) and, at 37 hpi, were often found in 'tight' phagolysosomal compartments. In contrast at 12 hpi, very few wild-type *M. marinum* were positive for CatD (arrowhead), but a population positive for vacuolin was emerging (arrows). At 37 hpi, wild-type *M. marinum* were very often found in apparently spacious (Vac)-positive compartments (asterisk) devoid of CatD, with elongated rods of bacteria sharply deforming the delimiting membranes of the vacuoles.
B. Close inspection during phase 2 revealed four sequential stages in the establishment and rupture of the vacuolin-positive vacuole. At the early stage 1, a single mycobacterium deformed a vacuole already enriched in vacuolin (black arrowheads). At stage 2, bacteria proliferation led to more deformation of the membrane (black arrowhead), whereas at the late stages 3 and 4, the vacuolin-positive membrane ruptured and bacteria were released to the cytosol (arrows). Arrowheads point to the edges of the membrane sheets generated during niche rupture.
C. The predicted copper transporter p80 was also enriched at the limiting membrane of the vacuole and visible on internal membranes. Scale bars, 10 μm for (A) (12 hpi) and 5 μm for (A) (37 hpi) and (B) and (C).

(Ravanel *et al*., 2001). Immunofluorescence staining of p80 during phase 2 of bacteria proliferation recapitulated the morphological stages 1–4, described above (Fig. 3C).

Brown and colleagues (Stamm *et al*., 2003) reported that 2 days after uptake into macrophages, *M. marinum* appeared in the cytosol; however, they did not observe directly the escape of *M. marinum* from its vacuole. As in macrophages, we also observed *M. marinum* in the cytosol in *Dictyostelium*. But, for the first time, we were able to capture intermediates of the rupture of the vacuole and to document the escape of the pathogen into the cytosol. A representative high-resolution example of a stage 3 vacuole rupture, obtained by three-dimensional reconstruction of confocal sections, is presented in Fig. 4. In the lower part of the cell, the vacuole membrane appeared intact with a normal patchy distribution of vacuolin (Fig. 4A, 1.6 μm). In sections higher up the cell, the vacuolin distribution appeared almost continuous

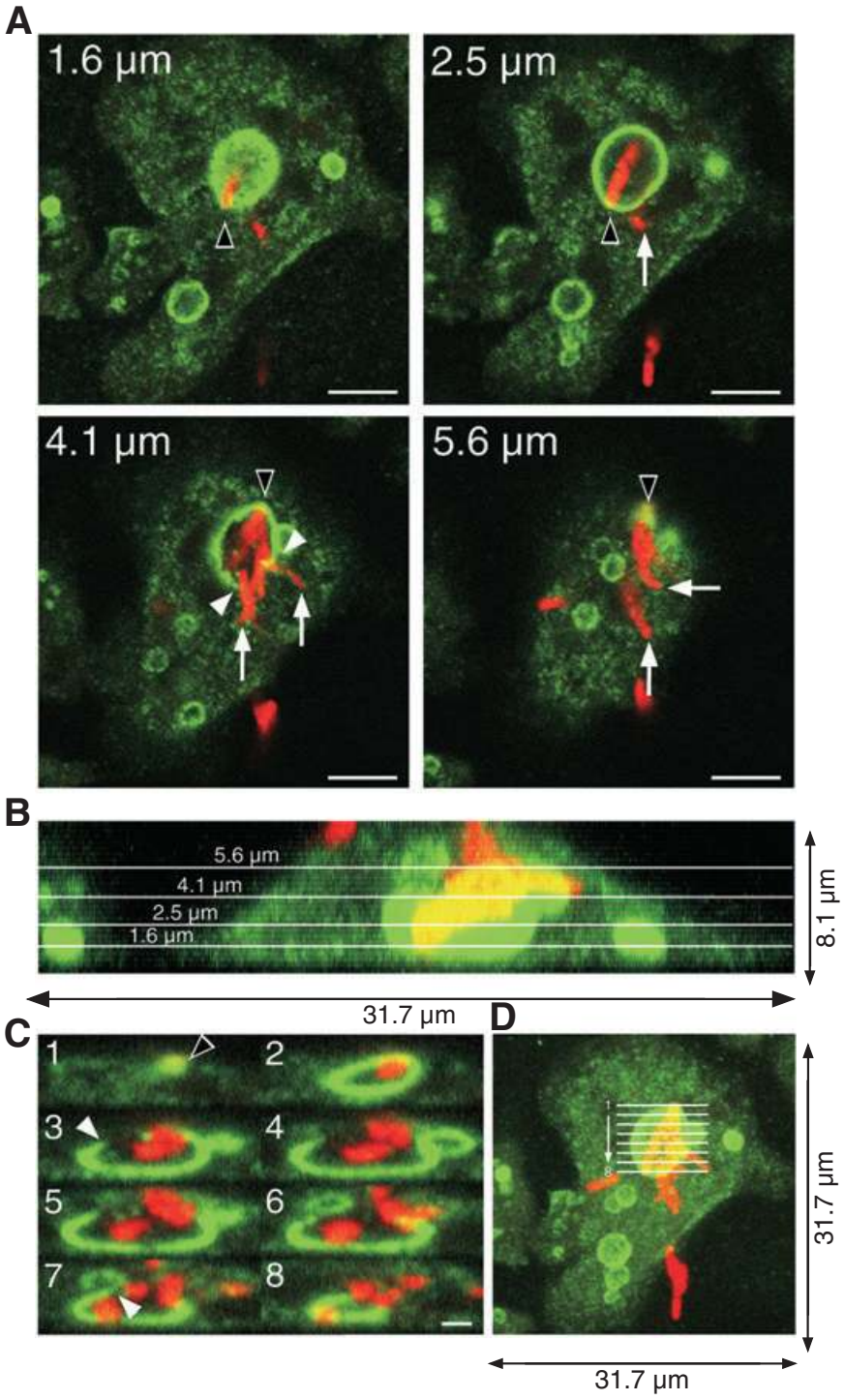

Fig. 4. Visualization of the rupture of a replication vacuole at high resolution. During phase 3 of infection by wild-type *M. marinum* (red), stable intermediates in the rupture of replication vacuoles, visualized by immunofluorescent staining against vacuolin (green), were frequently observed.

A. Four optical sections taken at various distances from the coverslip, as indicated in the upper left corner of each panel. Proliferating mycobacteria sharply deform the replication vacuole (black arrowheads), and escape to the cytosol (arrows) through breaches of the membrane. Arrowheads point to the edges of the broken vacuoles.

B. Three-dimensional reconstruction of the cell allows viewing along a vertical section. The positions of the four sections shown in (A) are indicated.

C and D. (C) Vertical sections (1–8) through the ruptured vacuole, at the positions indicated on top of the maximum projection shown in (D). Scale bars, 5 µm (A) and 1 µm (C).

(2.5 μm). Replicating bacterial rods appeared to deform the membrane and apparently broke through it, resulting in the opening at the top of the vacuolin-positive vacuole (4.1 and 5.6 μm). This was also seen in vertical sections through the reconstruction (Fig. 4C and D). The large number of rupturing proliferation niches we observed indicate that the vacuole remnants have a relatively long half-life.

Flotillin-1 accumulates at the replication niche in human monocytes

To test whether the accumulation of flotillin on the *M. marinum* replication niche occurs during infection of other organisms, we performed immunofluorescence staining on infected human peripheral blood monocytes. Healthy and proliferating *M. marinum* were distinguished from dead or dying bacteria by the strong accumulation of GFP fluorescence (Fig. 5). Phagosomes containing non-fluorescent or faintly fluorescent bacteria (faint blue, Fig. 5A and C) colocalized with LBPA, Lamp-1 and flotillin-1, three markers of a mycobactericidal phagolysosome (Fig. 5A and C). In contrast, highly fluorescent bacteria (bright blue, Fig. 5B and D) were found to proliferate in a compartment strongly positive only for flotillin-1 (Fig. 5B and D). LBPA seemed completely absent and Lamp-1 at the limit of detection. The distribution of flotillin-1 on the membrane was patchy, like that observed for vacuolin (compare Fig. 5 and Figs 3 and 4). We conclude that, as in *Dictyostelium*, flotillin accumulation is a marker of the proliferation niche of *M. marinum* in monocytes. Moreover, multiplication inside the monocyte vacuole also led to its deformation and was followed by rupture, in stages resembling those observed in *Dictyostelium* (Fig. 5E).

Host mutations have a profound impact on the course of infection

We wanted to determine whether the accumulation of vacuolin at the replication niche was necessary for establishing a mycobacteria-friendly compartment. So, we tested three well-studied *Dictyostelium* mutants, two of which have disordered vacuolin distribution and alterations in the morphology of the late endosomal compartments, but otherwise exhibit no severe growth, phagocytosis or exocytosis defect (see *Discussion* for more details). The mutants lacked vacuolin A (*vacA*$^-$), vacuolin B (*vacB*$^-$) or the RacH GTPase (*racH*$^-$) (Jenne *et al*., 1998; Somesh *et al*., 2006).

To characterize the early response of the pathogen, we first investigated activation of the map24 promoter. As in wild-type cells (Fig. 1D), the *M. marinum* map24 promoter was activated in all three mutant cell lines (Fig. 6): GFP was detected at 3 hpi and increased further during the first 9 hpi. We noted that in *racH*$^-$ cells, strong GFP fluorescence was detected earlier than in wild-type cells. These data indicate that the pathogen's 'infection programme' was activated inside each of these mutant hosts.

The course of infection was monitored by counting cfu and by FACS analysis. Initial uptake of *M. marinum* by all three strains was similar (Fig. 7A and B, at 0.5 hpi), but the infections had different outcomes. In *vacA*$^-$ cells, the temporal profiles and extent of intracellular proliferation measured by cfu were indistinguishable from wild-type *Dictyostelium* (Fig. 7A), and FACS analysis revealed a persistent population of infected cells that gradually increased in fluorescence (Fig. 7B). In *vacB*$^-$ cells, no net proliferation was observed (Fig. 7A): in some experiments the number of cfu decreased, whereas in others it was relatively stable, but the size of the population of infected cells clearly decreased, as shown by FACS analysis (Fig. 7B). In *racH*$^-$ cells, there was significantly more proliferation of *M. marinum* than in wild-type *Dictyostelium* (Fig. 7A): cfu counts were more stable in phase 1 and rose more steeply in phase 2, with around 50% more cfu at 37 hpi than in wild-type cells. There was only a minimal or undetectable decrease in cfu during phase 3 in the *racH*$^-$ cells. FACS analysis confirmed these findings (Fig. 7B). As in wild-type and *vacA*$^-$ cells, the population of infected *racH*$^-$ cells persisted throughout the experiment but, in sharp contrast to the former two, the entire population gradually shifted to higher FL1 and SSC values due to more accumulation of fluorescent bacteria (Fig. 7B).

The fate of the intracellular bacteria was also different in each cell line. Whereas in *vacA*$^-$ cells bacteria were observed escaping a cathepsin D-negative and vacuolin B-positive proliferation vacuole, in *vacB*$^-$ cells, most were found in a bloated compartment that was cathepsin D- and/or vacuolin A-positive, characteristic of late endosomal compartments in that mutant strain (Jenne *et al*., 1998) (Fig. 7C). Immunofluorescence staining of VatA revealed that, contrary to the situation in wild-type cells, in *vacB*$^-$ cells the vacuolar H^+-ATPase accumulated around bacteria during phase 1, reaching a peak of 56% VatA-positive vacuoles at 12 hpi (Fig. 7D and E), suggesting that most bacteria were directed to a mycobactericidal environment. Despite this, a few bacteria were seen in the cytosol of *vacB*$^-$ cells, indicating a low level of proliferation and escape from the vacuole. We conclude that, in the absence of vacuolin B, cells are overall more resistant to infection because a low level of pathogen proliferation is balanced by increased killing of the bacteria in phagolysosomes. In *racH*$^-$ cells, although the distribution of vacuolin and the morphology of late endosomes are perturbed, *M. marinum* established a vacuolin-positive replication niche (Fig. 7C). Also, as in wild-type cells, the vacuole in *racH*$^-$ cells ruptured and bacteria were released into the cytosol (Fig. 7C). Despite these

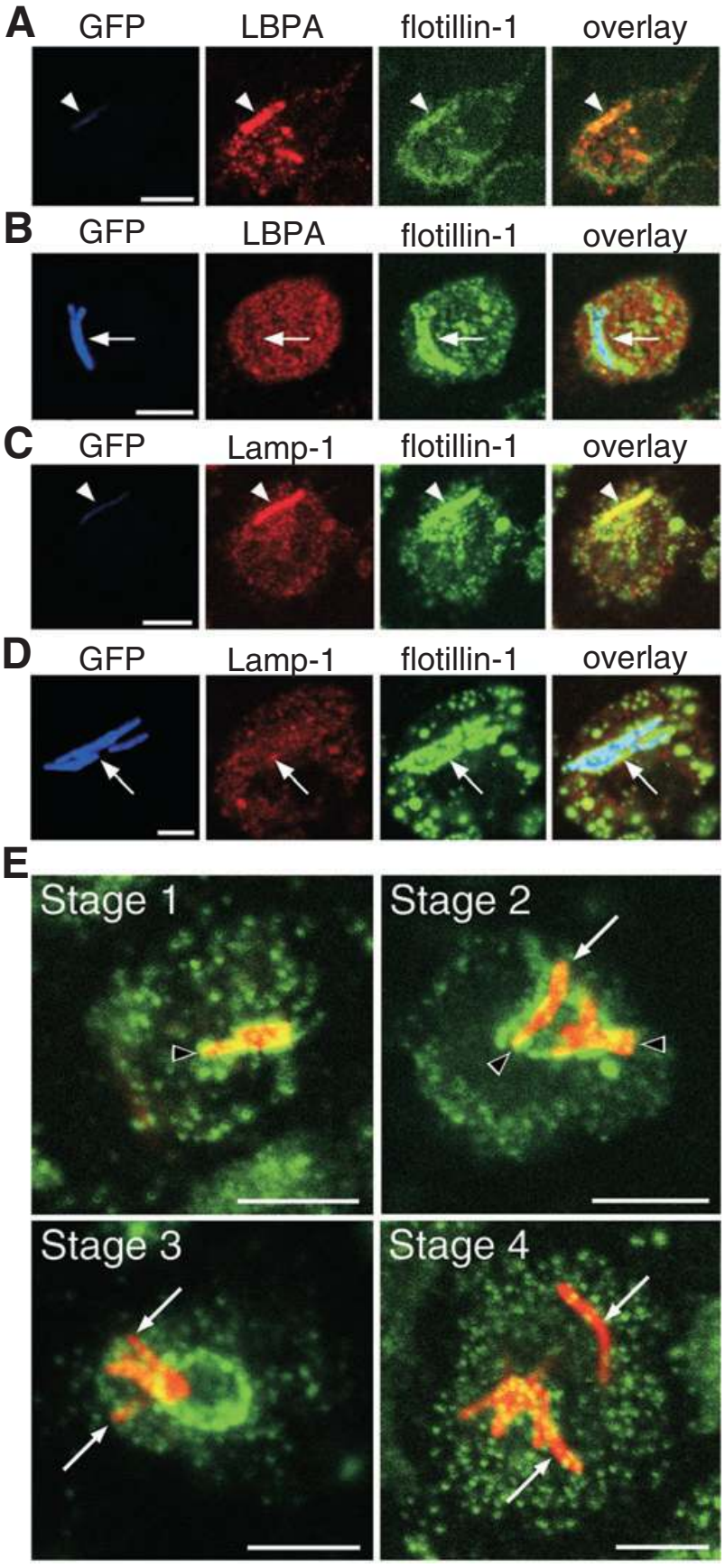

Fig. 5. Flotillin is a marker of the replication niche for *M. marinum* in peripheral blood monocytes. Uptake of wild-type *M. marinum* in adherent human peripheral blood monocytes was performed as described for *Dictyostelium* cells in Fig. 1.
A–D. Phagosomes containing dead or dying non-fluorescent or faintly fluorescent bacteria (A, C, faint blue), colocalized with LBPA (A, red), Lamp-1 (C, red) and flotillin-1 (A–D, green), markers of a bactericidal phagolysosome. In contrast, healthy and proliferating highly fluorescent bacteria (B, D, bright blue) were found in compartments positive for flotillin-1 (B, D, green) but not for LBPA (B, red) or for Lamp-1 (D, red).
E. Multiplication inside a flotillin-1-positive vacuole (green) also led to its deformation and rupture, in stages 1–4 resembling those observed in *Dictyostelium* (compare with Fig. 3B). The distribution of flotillin-1 on the membrane was as patchy as that observed for vacuolin (compare with Figs 3 and 4). Scale bars, 5 μm.

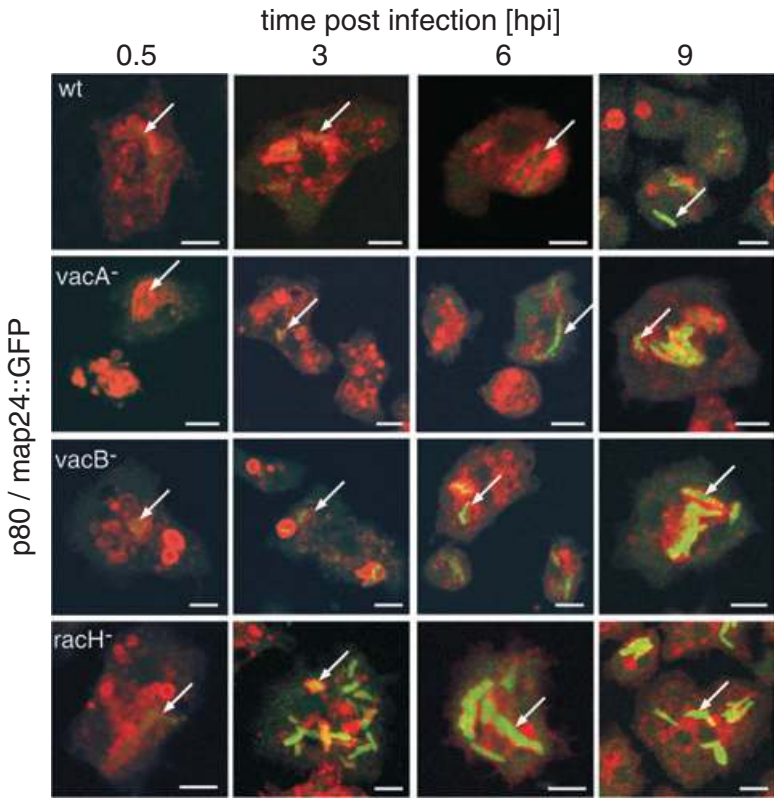

Fig. 6. The map24 promoter is activated in *M. marinum* during infection of three *Dictyostelium* mutant strains. Wild type, *vacA*$^-$, *vacB*$^-$ and *racH*$^-$*Dictyostelium* cells were infected with wild-type *M. marinum* carrying the map24::GFP vector. At the indicated times, cells were stained for the p80 marker (red). Arrows point to GFP-expressing fluorescent mycobacteria (that were also stained by DAPI, not shown), revealing GFP accumulation (green) in all strains as early as 3 hpi. GFP expression was visible earlier and accumulated to higher levels in *M. marinum*-infected *racH*$^-$ cells. Scale bars, 5 μm.

similarities in the intracellular course of the infection, *racH*$^-$ cells allow more efficient *M. marinum* proliferation.

Finally, FACS analysis of infected cultures of wild-type and the two vacuolin mutant cell lines revealed a prominent population of bacteria released from the host cells (Fig. 7B). Strikingly, this population of extracellular bacteria was almost completely absent from infected cultures of *racH*$^-$ cells. It thus appears that the absence of RacH has an impact on bacteria release and cell-to-cell transmission of the infection.

Discussion

Altogether our data indicate that a cycle of infection by pathogenic *M. marinum* in *Dictyostelium* can be defined by three phases: establishment of an infection niche, intracellular proliferation of the pathogen and release of the pathogen from the host cell (Fig. 8). This release results in infection of neighbouring cells to start new cycles whose integration over time leads to an increase of the number of infected cells and exponential growth of bacteria in the infected culture (our own unpublished data, and reported in Solomon *et al*., 2003). If the bacteria were simply released into the medium, reinfection should be completely sensitive to extracellularly applied antibiotics. This is not the case in our experiments, which confirms previous reports of *M. marinum* infection in macrophages (Stamm *et al*., 2003) and has also been described for *M. tuberculosis* in a fibroblast microcolony assay (Byrd *et al*., 1998). This may reflect an uncharacterized but specific cell-to-cell transmission mechanism in which bacteria are only briefly or not at all exposed to the extracellular antibiotics.

We show here that in *Dictyostelium*, as in other hosts (Ramakrishnan *et al*., 2000; Dionne *et al*., 2003), pathogenic *M. marinum* bypasses phagosome maturation to establish a 'friendly' environment for replication, and that non-pathogenic *M. smegmatis* is efficiently killed by *Dictyostelium*. During the very early steps in the establishment of infection, we observed the transient presence of the vacuolar H^+-ATPase in the compartments containing pathogenic mycobacteria. These results are compatible with earlier seminal reports (Sturgill-Koszycki *et al*., 1994). It was found that phagosomes containing mycobacteria, isolated at 30 min to 4 days post infection, had undetectable levels of H^+-ATPase. However, pH measurement revealed a mild acidification, already visible at 30 mpi. This was proposed to result from either inhibition of delivery or from a rapid removal of the H^+-ATPase. Thus, our observation of very early and transient recruitment of the H^+-ATPase strongly supports the second model.

Furthermore, during this early phase, the accumulation of p80, a late phagosomal marker, in the vacuole surrounding wild-type *M. marinum* was delayed and more gradual compared with phagosomes containing

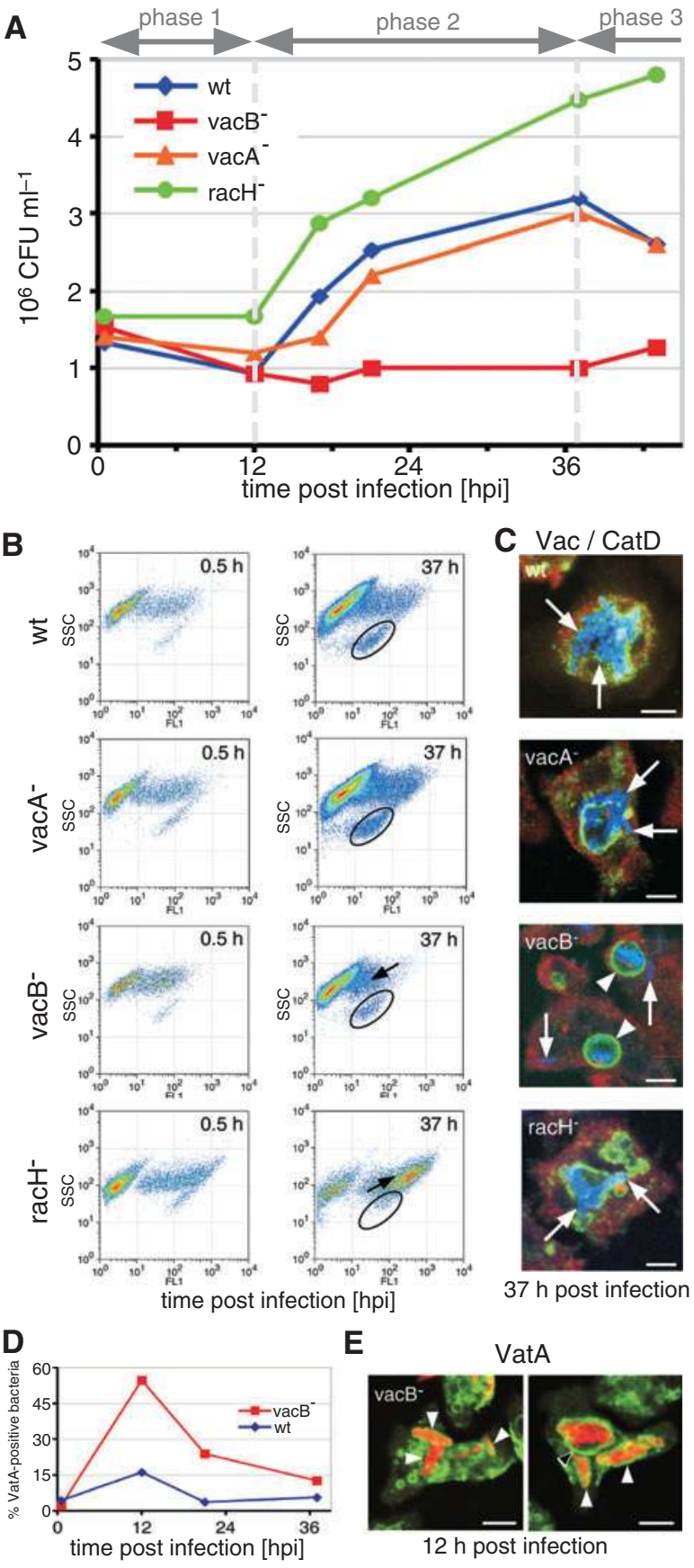

Fig. 7. Fate of wild-type *M. marinum* during infection of three *Dictyostelium* mutants. Uptake of wild-type *M. marinum* in wild type, *vacA*⁻, *vacB*⁻ and *racH*⁻ *Dictyostelium* cells was performed as in Fig. 1.
A and B. At the indicated times, the concentration of live mycobacteria was measured by counting cfu (A), and the dynamics of the populations in the infection mix were monitored by FACS (B) as in Fig. 1. (A) Proliferation of *M. marinum* was very similar in wild-type and *vacA*⁻ cells, and followed the three phases described in Fig. 1. No significant overall increase in the number of live bacteria was detectable in *vacB*⁻ cells. In contrast, in *racH*⁻ cells mycobacteria proliferated earlier and more robustly, and no clear phase 3 was discernible. (B) FACS analyses confirmed that, at 37 hpi, a population of infected cells persisted in wild-type and *vacA*⁻ cells, but had almost completely disappeared from *vacB*⁻ cells (downward-pointing arrow). In contrast again, high levels of proliferation were seen in *racH*⁻ cells, resulting in a shift to higher SSC and FL1 values (upward-pointing arrow). Extracellular fluorescent mycobacteria (circles) were released from all except the *racH*⁻ cells, confirming the lack of a phase 3.
C. Representative examples of the four strains of cells infected by fluorescent *M. marinum* (blue), taken at 37 hpi and stained for vacuolin (Vac, green) and cathepsin D (CatD, red). Rupture of vacuolin-positive proliferation vacuoles and bacteria present in the cytosol (arrows) can be frequently seen in infected cells from every strain except *vacB*⁻, in which the mycobacteria were mostly found in enlarged phagolysosomal compartments that stained positive for vacuolin and cathepsin D (arrowheads).
D and E. Wild-type and *vacB*⁻ cells were infected with GFP-expressing wild-type *M. marinum* and, at the indicated times, were scored for the presence of VatA. Quantification (D) and representative examples at 12 hpi (E) indicated that in *vacB*⁻ cells, the majority of mycobacteria (red) colocalized with VatA (green, white arrowheads) and were sometimes in unusually spacious vacuoles (black arrowhead) that resemble late endolysosomal vacuoles in *vacB*⁻ cells (Jenne *et al*., 1998). Scale bars, 5 μm (C and E).

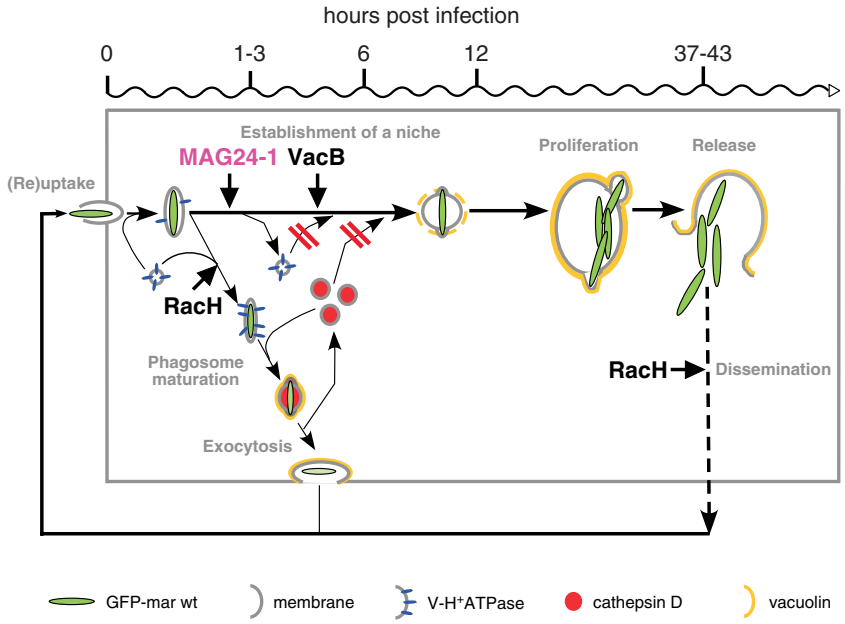

Fig. 8. Schematic representation of the fate of pathogenic *M. marinum* during establishment, maintenance and cell-to-cell spreading of an infection in *Dictyostelium*. Uptake of *M. marinum* by *Dictyostelium* results in the formation of a phagosome that transiently acquires the early marker vacuolar H^+-ATPase. Further maturation is bypassed (indicated by a bold arrow), the level of vacuolar H^+-ATPase becomes undetectable and delivery of cathepsin D (interrupted arrows) is blocked. However, the vacuole gradually accumulates vacuolin on its cytoplasmic surface (12–37 hpi). Subsequent to intravacuolar proliferation of the mycobacteria (12–37 hpi) the vacuolin coated and p80 positive-compartment ruptures and the bacteria are released into the host cytosol (37–43 hpi). The presence of the pathogen protein MAG24-1 and the host protein vacuolin B are crucial for efficient establishment and/or maintenance of the replication niche. A minority of bacteria (indicated by a light arrow) follows the normal degradative phagosomal route, and their vacuoles mature normally. The presence of RacH increases the number of bacteria following this pathway, thus rendering the host cells more immune to infection. The overall fate of an infection is thus a balance between the two pathways. It is unclear how the pathogen is released from its host and spreads from cell to cell, but RacH is essential for this process.

M. smegmatis and *M. marinum* L1D. This is best explained by a bifurcation from the standard maturation programme, but suggests at the same time that the forming replication niche remains fusogenic and has interactions, even though limited, with the endocytic pathway of the host cell, as already reported for pathogenic mycobacteria in macrophages (Sturgill-Koszycki *et al.*, 1996).

Furthermore, we show that the *M. marinum* map24 promoter is activated early after phagocytosis, and that the gene product it regulates, MAG24-1, is crucial for efficient infection. Indeed, phagosomes containing the mutant *M. marinum* L1D, which does not express MAG24-1, undergo maturation in *Dictyostelium* like phagosomes containing any inert particle or non-infectious bacterium and are exocytosed within 1–3 hpi (see Fig. S1 in *Supplementary material*). Thus, our findings suggest that, as reported for specific mycobacterial lipids (Fratti *et al.*, 2003; Vergne *et al.*, 2004b) the *M. marinum* PE-PGRS protein MAG24-1 plays an important role in initiating the phagosome maturation bypass. We speculate that MAG24-1 is important to limit or revert the transient delivery of the V-ATPase and that other proteins of the PE and PPE families might play similar roles in the pathogenesis induced by other mycobacteria.

Little is known about the composition of the mycobacteria replication vacuole (Russell, 2001). Here, we show that at the onset of intravacuolar replication (phase 2 in Fig. 1 and 12–37 hpi in Fig. 8) two host proteins, vacuolin and p80, accumulate at the pathogen-containing vacuole. It is interesting to note that this vacuole acquires some of the characteristics of the neutral post-lysosomal compartment, but its biogenesis bypasses the standard and strict maturation programme. In addition, it also dramatically differs in function, as the post-lysosomes normally recruit coronin and undergo actin-dependent exocytosis (Maniak, 2003), while these markers are not significantly associated with the *M. marinum* replication niche (data not shown). We also demonstrate that the human vacuolin homologue, flotillin, accumulates around proliferating *M. marinum* in peripheral blood monocytes. We thus speculate that formation of the replication niche for pathogenic mycobacteria, including *M. tuberculosis*, in mammalian macrophages proceeds along a similar route as in *Dictyostelium* to reach a flotillin-positive, quasi-neutral compartment partly connected to the endosomal system.

Interestingly, other pathogens have been shown to interfere with the localization of flotillins during establishment of an infection. The protozoan *Leishmania donova-*

nii, for example, prevents delivery of flotillin-1 to its replication compartment (Dermine *et al*., 2001), in contrast to the intracellularly replicating bacterium, *Brucella*, that induces increased and sustained recruitment of flotillin-1 to its replication compartment (Arellano-Reynoso *et al*., 2005). The parasite *Plasmodium falciparum* is even known to export its own orthologue of stomatin, another member of the extended flotillin family, into its host erythrocyte during the development of the parasitophorous vacuole (Hiller *et al*., 2003). It remains to be understood why flotillins appear to be a common target for various intracellular pathogens.

Although the exact biochemical functions of vacuolin and flotillin are unknown, their structural similarities to caveolin and reticulon suggest they play a role in scaffolding membrane domains (Bauer and Pelkmans, 2006). If so, recruitment of a dense vacuolin coat onto the replication niche might influence its fusion/fission properties, altering trafficking of 'bactericidal' proteins (such as the H^+-ATPase and hydrolases) to and from the vacuole.

We found that the putative copper transporter, p80 (Ravanel *et al*., 2001), also accumulates in the pathogen replication vacuole. It is well known that copper and iron are toxic at high concentrations but are vital to mycobacteria: the *M. tuberculosis* copper-dependent enzyme SodC is essential to eliminate the superoxide produced during the oxidative burst in macrophages (Piddington *et al*., 2001), and iron is an essential cofactor for metabolic enzymes. By homology with other copper transporters (Nose *et al*., 2006), p80 is expected to transport copper out of the vacuole into the cytosol, a role similar to the divalent metal cation transporter Nramp1 that pumps iron out of the vacuole (Peracino *et al*., 2006). Control of ion homoeostasis through the active recruitment or depletion of specific transporters thus appears to be important in establishing a friendly environment for mycobacteria proliferation.

Very few host factors that modulate mycobacteria infection are known, but, for example, a recent genome-wide RNAi screen on *Drosophila* phagocytic-like cells revealed host genes that are specifically needed for *Mycobacterium fortuitum* infection (Philips *et al*., 2005). Here, we show for the first time that, in the absence of the flotillin homologue vacuolin B, pathogenic mycobacteria are unable to prevent accumulation of the H^+-ATPase and thus fail to establish a safe proliferation niche. This function is specific for this isoform because the absence of vacuolin A, which is 77% identical to vacuolin B and forms heteromultimers with it (Wienke *et al*., 2006), had no measurable effect on accumulation of the H^+-ATPase. Our study also revealed an important role for a GTPase in the establishment of infection (Fig. 8). Interestingly, *racH*$^-$ cells, which are known to exhibit alterations in the vacuolin-positive compartment, were more susceptible than wild-type cells to *M. marinum* infection. The endocytic transit time is reported to be prolonged in both *vacB*$^-$ and *racH*$^-$ cells (Jenne *et al*., 1998; Somesh *et al*., 2006); however, whereas endolysosome acidification is prolonged in *vacB*$^-$ cells (Jenne *et al*., 1998), it is drastically reduced in *racH*$^-$ cells (Somesh *et al*., 2006). Instead of the transient recruitment of the vacuolar H^+-ATPase observed in wild-type cells, we suggest that, upon uptake in *vacB*$^-$ cells, *M. marinum* is exposed to a lower pH for a prolonged period of time, thus contributing to the higher resistance of *vacB*$^-$ cells to infection. Vice versa, the quasi-absence of early phagosomes acidification in *racH*$^-$ cells contributes to the increased success of *M. marinum* in establishing a proliferation niche and replicating.

Even in *vacB*$^-$ cells, in which *M. marinum* does not proliferate efficiently, the map24 promoter is switched on. We interpret this as a sign that the pathogen's 'infection programme' is activated. In *racH*$^-$ cells, the earlier and more robust activation of the map24 promoter likely results in increased accumulation of MAG24-1, which might render the pathogen more efficient at bypassing maturation and establishing a safe niche (Fig. 8).

According to our model, a host impaired in acidification or weakened in general might allow proliferation of a weakened pathogen. The lack of acidification in *racH*$^-$ cells might give the avirulent mutant *M. marinum* L1D an advantage during the first hour after uptake to escape complete phagosomal maturation and proliferate. We therefore tested the efficiency of *M. marinum* L1D to establish an infection and proliferate in *racH*$^-$ cells (see Fig. S3 in *Supplementary material*). Overall the *racH*$^-$ cell line provided a better host for *M. marinum* L1D, as the bacteria were able to prevent their exocytosis and underwent less killing. However, *racH*$^-$ cells did allow only limited intracellular proliferation of *M. marinum* L1D compared with wild-type *M. marinum* in wild-type cells. Therefore, we conclude that the mutation in the host *racH* gene is only partially epistatic to the L1D mutation in the pathogen *M. marinum*.

By using vacuolin and flotillin as markers of the *M. marinum* proliferation niche in *Dictyostelium* and blood monocytes, respectively, we were able to follow the biogenesis and, ultimately, the rupture of the vacuole. The cause of the rupture is not known yet, but the observations of mycobacteria sharply deforming the vacuole membrane before it breaches suggest that mechanical forces play a role. Alternatively, it is possible that *M. marinum* uses a similar strategy to *Listeria* and *Shigella*, which escape the early phagosome by lysing its membrane enzymatically. Bloom and colleagues had documented rupture of the *M. tuberculosis*-containing vacuole by electron microscopy imaging (McDonough *et al*., 1993), but it was not until very recently that evidence was again presented showing that, in myeloid cells, *M. tuberculosis* and *M. leprae* translocate from their

vacuole to the cytosol (van der Wel *et al*., 2007). This translocation seems to be dependent on functional RD1 locus and ESAT-6 secretion (van der Wel *et al*., 2007). On the other hand, Brown and colleagues recently suggested that the *M. tuberculosis* and *M. marinum* protein ESAT-6, which is secreted by a system encoded in the RD1 locus, exhibits a membranolytic activity responsible for the haemolytic and cytolytic activities that are reported to play a role in bacterial spreading (Gao *et al*., 2004). We would like to speculate that the membranolytic activity might actually serve to lyse both the vacuole and the plasma membrane.

In our system, proliferation of *M. marinum* clearly occurred in the vacuole, and it remains to be determined whether it also occurred in the cytosol after vacuole rupture. In myeloid cells, there are indications for proliferation in the cytosol (van der Wel *et al*., 2007). It is truly puzzling that, after establishing and maintaining a safe niche for proliferation, the bacteria are released into the cytosol, a biochemically and metabolically completely different environment.

Although in *Dictyostelium* and in human blood monocytes we clearly documented vacuole rupture, we did not observe actin tails on cytosolic *M. marinum.* But such actin tails were clearly seen in infected BV2 microglial cell (our unpublished observation). Again, in myeloid cells, no actin tail formation was detected on cytosolic *M. tuberculosis* and *M. leprae* (van der Wel *et al*., 2007).

In *Dictyostelium* and in human blood monocytes, the long half-life of remnants of the ruptured vacuole was surprising because, naïvely, one might expect a ruptured endomembrane compartment to disappear like a burst soap bubble. We hypothesize that the replication vacuole membrane is stabilized either by the densely packed vacuolin/flotillin coat, or by the biophysical properties conferred by the coalescence of flotillin–lipid rafts. The patchy distribution of vacuolin and flotillin is, indeed, suggestive of membrane microdomains.

In the light of the latest evidence, vacuole rupture and the presence of pathogenic mycobacteria in the cytosol might well represent a general strategy to ensure successful infection. If confirmed, it would raise further fundamental questions for future research. Does vacuole rupture and subsequent release of antigens directly into the cytosol modulate antigen (cross)-presentation (Grode *et al*., 2005)? Is autophagy of cytosolic pathogens involved in controlling pathogenesis (Vergne *et al*., 2006)? Finally, does escape from the vacuole play a role in cell-to-cell spreading?

Relevant to this latter point, our FACS analysis revealed that infected *racH*$^-$ cells accumulated very large numbers of fluorescent mycobacteria. The frequent presence of over 30–50 bacteria per cell was confirmed by fluorescence microscopy (our unpublished observations). In addition, strikingly, almost no extracellular bacteria were detected, which corroborates the apparent lack in cfu graphs of a phase 3 of bacteria release and killing. These data provide the strongest clue that there may be a dedicated mechanism for mycobacteria release from the host cell after proliferation; the importance of the RacH GTPase in this process is the first step towards the molecular characterization of such a mode of cell-to-cell transmission.

Experimental procedures

Cell culture

Wild-type *Dictyostelium discoideum* (Ax2) was cultivated axenically at 22°C in HL5c medium (Formedium). M. Maniak (Kassel University, Germany) provided the *vacA*$^-$ and *vacB*$^-$ strains. F. Rivero (Cologne University, Germany) provided the *racH*$^-$ strain.

Mycobacteria strains, culture and plasmids

Mycobacteria were cultured in Middlebrook 7H9 (Difco) supplemented with 10% OADC (Becton Dickinson), 5% glycerol and 0.2% Tween80 (Sigma Aldrich) at 32°C in shaking culture. *M. smegmatis* was a gift from G. Griffiths (EMBL, Heidelberg, Germany). L. Ramakrishnan (Washington University, Seattle, USA) provided *M. marinum* wild type, *M. marinum* L1D, and the msp12::GFP and map24::GFP plasmids. *M. marinum* and *M. smegmatis* strains expressing GFP in a constitutive or regulated fashion were obtained by transformation with msp12::GFP or map24::GFP vectors, respectively, and cultivated in the presence of 20 μg ml^{-1} kanamycin.

Infection assay

Mycobacteria were grown to a density of ~OD_{600} = 1.0 (~5×10^8 bacteria ml^{-1}), washed twice in HL5c medium and clumps disrupted by passaging through a 26-gauge needle. A total of 5×10^7 wild-type or mutant *Dictyostelium* cells were plated onto 10 cm dishes and allowed to adhere for 20 min at 25°C. Bacteria were added at an moi of 10 and centrifuged onto the *Dictyostelium* cells at 500 *g* twice for 10 min. The cells were left at 25°C for an additional 10–20 min before uningested bacteria were washed off by five washes with HL5c. Attached cells were then re-suspended in 37.5 ml of HL5c containing 5 μg ml^{-1} streptomycin. The infected culture was incubated with shaking (130 r.p.m.) at 25°C for up to 5 days. The concentration of streptomycin (5 μg ml^{-1}) was adjusted to completely inhibit extracellular proliferation of bacteria, but to be permissive for intracellular bacteria growth, confirming a previous report (Solomon *et al*., 2003). We defined the time post infection relative to the moment when the bacteria were added to the attached cells. The first sample was taken when the uningested, extracellular bacteria were removed, which was approximately 30 mpi (0.5 hpi). For the short infection experiments (5–90 mpi), we plated *Dictyostelium* cells on coverslips and infected them with mycobacteria at an moi of 20 by centrifuging at 500 *g* for 5 min. Extracellular, uningested bacteria were washed off and samples were fixed immediately (corresponding to 5 mpi), and at 20 mpi and 90 mpi.

Colony-forming unit measurements

The number of viable bacteria was determined by analysing 300 μl aliquots of infected culture. Cells were washed with PBS, and lysed for 10 min in PBS with 0.1% Triton-X100. Serial dilutions in lysis buffer were plated onto Middlebrook 7H11 plates (Difco) and incubated at 32°C for 5–7 days.

Flow cytometry assays

To analyse host and pathogen population dynamics in infected cultures, *Dictyostelium* cells were infected with GFP-expressing bacteria. Aliquots of 500 μl were taken at the indicated times and diluted with 500 μl of Sørensen buffer (14.7 mM KH_2PO_4, 2.5 mM $NaHPO_4$, pH 6.2) containing 5 mM sodium azide to strip the cell surface of loosely attached bacteria. Cells were pelleted 4 min at 14 000 r.p.m. and re-suspended in 500 μl of Sørensen containing 20 mM sorbitol and kept on ice. Immediately before counting, fluorescent latex beads (100 beads μl^{-1}, 4.5 μm of YG-beads, Molecular Probes) were added as an internal particle concentration standard. Flow cytometry was performed on a FACScalibur (Beckton Dickinson) and data were analysed with FlowJo (TreeStar, USA).

Isolation, culture and infection of peripheral blood monocytes

Monocytes were isolated from human blood using the Accuspin-system Histopaque-1077 (Sigma Aldrich) as described by the manufacturer. For infection, the cells were re-suspended in RPMI1460-Glutamax medium (Gibco) and allowed to adhere to polylysine-coated coverslips. GFP-expressing *M. marinum* were washed twice with RPMI1460-Glutamax medium and added to the cells at an moi of 1. Bacteria were centrifuged onto attached cells for 15 min at 500 *g*. The cells were allowed to phagocytose for 2 h at 32°C with 5% CO_2. Extracellular bacteria were washed off and the cells maintained in medium supplemented with 20% fetal calf serum, 25 mM Hepes and 5 μg ml^{-1} streptomycin at 32°C with 5% CO_2. After 43 h, the coverslips were rinsed in PBS and cells fixed with 4% paraformaldehyde in PBS.

Antibodies and fluorescent reagents

Antibodies against the following antigens were obtained from: Cathepsin D (CatD; Journet *et al*., 1999) from J. Garin (CEA, Grenoble, France); VatA (Neuhaus *et al*., 1998) and vacuolins (221-1-1; Rauchenberger *et al*., 1997) from M. Maniak (Kassel University, Germany); p80 (Ravanel *et al*., 2001) from P. Cosson (University of Geneva, Switzerland); flotillin-1 (Fivaz *et al*., 2002) from G. van der Goot (EPFL, Lausanne, Switzerland); LBPA (6C4; Kobayashi *et al*., 1998) and Lamp-1 (4A1; Aniento *et al*., 1993) from J. Gruenberg (University of Geneva, Switzerland). It is important to mention that three vacuolin isoforms are encoded in the genome (VacA, VacB and the unstudied VacC), two of which (VacA and VacB) are expressed in vegetative cells. The antibody used in this study to detect vacuolin does not distinguish between the two isoforms (VacA and VacB) and presumably can also recognize VacC. Secondary antibodies were goat anti-mouse or goat anti-rabbit IgG coupled to Alexa488 or Alexa594 (Molecular Probes), and Cy5 (Rockland).

Immunofluorescence

Dictyostelium cells infected with wild type, mutant or GFP-expressing mycobacteria were fixed by rapid freezing and immunostained exactly as described (Hagedorn *et al*., 2006). Immunofluorescence images were documented with a Leica SP2 confocal microscope using a 100× 1.4NA oil-immersion objective. Recording parameters for fields of 1024 × 1024 pixels with appropriate electronic zoom (2–8×) were 4 × line-averaging and 0.1–0.32 μm vertical steps.

Quantification

The proportion of infected cells and the number of GFP-expressing bacteria per cell was determined after immunofluorescent labelling against p80 to distinguish cell-associated bacteria. To monitor the level of infection, a minimum of three fields were counted. The number of intracellular bacteria was determined in a minimum of 100 *Dictyostelium* cells, on a minimum of five optical sections, for each time point. For colocalization with maturation markers, z-stacks were recorded through a minimum of 100 infected *Dictyostelium* cells and the number of bacteria present in labelled compartments was scored. These quantifications were performed independently for the VatA subunit of the vacuolar H^+-ATPase, for p80 and vacuolin. Data were analysed and graphed using Prism (GraphPad) and Excel (Microsoft office).

Acknowledgements

We gratefully acknowledge Lalita Ramakrishnan and Christine Cosma for providing strains of *M. marinum*, various GFP-expression vectors and advice; Gisou van der Goot and Jean Gruenberg for providing various antibodies; Gareth Griffiths for providing *M. smegmatis*; Francisco Rivero and Markus Maniak for providing *Dictyostelium* mutant strains; Jonathan Matthews for his preliminary studies and Siouxsie Wiles and Brian Robertson in Douglas Young's lab for their help at the start of the project. The Swiss National Science Foundation supported this work. Our group participates in the NEMO (non-mammalian experimental models for the study of bacterial infections) network supported by the Swiss 3R Foundation.

References

Aniento, F., Emans, N., Griffiths, G., and Gruenberg, J. (1993) Cytoplasmic dynein-dependent vesicular transport from early to late endosomes. *J Cell Biol* **123:** 1373–1387.

Arellano-Reynoso, B., Lapaque, N., Salcedo, S., Briones, G., Ciocchini, A.E., Ugalde, R., *et al.* (2005) Cyclic beta-1,2-glucan is a *Brucella* virulence factor required for intracellular survival. *Nat Immunol* **6:** 618–625.

Barker, L.P., George, K.M., Falkow, S., and Small, P.L. (1997) Differential trafficking of live and dead *Mycobacterium marinum* organisms in macrophages. *Infect Immun* **65:** 1497–1504.

Bauer, M., and Pelkmans, L. (2006) A new paradigm for membrane-organizing and -shaping scaffolds. *FEBS Lett* **580:** 5559–5564.

Byrd, T.F., Green, G.M., Fowlston, S.E., and Lyons, C.R. (1998) Differential growth characteristics and streptomycin susceptibility of virulent and avirulent *Mycobacterium tuberculosis* strains in a novel fibroblast-mycobacterium microcolony assay. *Infect Immun* **66:** 5132–5139.

Cosma, C.L., Klein, K., Kim, R., Beery, D., and Ramakrishnan, L. (2006) *Mycobacterium marinum* Erp is a virulence determinant required for cell wall integrity and intracellular survival. *Infect Immun* **74:** 3125–3133.

Cosson, P., Zulianello, L., Join-Lambert, O., Faurisson, F., Gebbie, L., Benghezal, M., *et al.* (2002) *Pseudomonas aeruginosa* virulence analyzed in a *Dictyostelium discoideum* host system. *J Bacteriol* **184:** 3027–3033.

Dermine, J.F., Duclos, S., Garin, J., St-Louis, F., Rea, S., Parton, R.G., and Desjardins, M. (2001) Flotillin-1-enriched lipid raft domains accumulate on maturing phagosomes. *J Biol Chem* **276:** 18507–18512.

Dionne, M.S., Ghori, N., and Schneider, D.S. (2003) Drosophila melanogaster is a genetically tractable model host for Mycobacterium marinum. *Infect Immun* **71:** 3540–3550.

Ferrari, G., Langen, H., Naito, M., and Pieters, J. (1999) A coat protein on phagosomes involved in the intracellular survival of mycobacteria. *Cell* **97:** 435–447.

Fivaz, M., Vilbois, F., Thurnheer, S., Pasquali, C., Abrami, L., Bickel, P.E., *et al.* (2002) Differential sorting and fate of endocytosed GPI-anchored proteins. *EMBO J* **21:** 3989–4000.

Fratti, R.A., Chua, J., Vergne, I., and Deretic, V. (2003) *Mycobacterium tuberculosis* glycosylated phosphatidylinositol causes phagosome maturation arrest. *Proc Natl Acad Sci USA* **100:** 5437–5442.

Gao, L.Y., Groger, R., Cox, J.S., Beverley, S.M., Lawson, E.H., and Brown, E.J. (2003a) Transposon mutagenesis of *Mycobacterium marinum* identifies a locus linking pigmentation and intracellular survival. *Infect Immun* **71:** 922–929.

Gao, L.Y., Guo, S., McLaughlin, B., Morisaki, H., Engel, J.N., and Brown, E.J. (2004) A mycobacterial virulence gene cluster extending RD1 is required for cytolysis, bacterial spreading and ESAT-6 secretion. *Mol Microbiol* **53:** 1677–1693.

Gao, L.Y., Pak, M., Kish, R., Kajihara, K., and Brown, E.J. (2006) A mycobacterial operon essential for virulence *in vivo* and invasion and intracellular persistence in macrophages. *Infect Immun* **74:** 1757–1767.

Gotthardt, D., Warnatz, H.J., Henschel, O., Bruckert, F., Schleicher, M., and Soldati, T. (2002) High-resolution dissection of phagosome maturation reveals distinct membrane trafficking phases. *Mol Biol Cell* **13:** 3508–3520.

Gotthardt, D., Blancheteau, V., Bosserhoff, A., Ruppert, T., Delorenzi, M., and Soldati, T. (2006) Proteomic fingerprinting of phagosome maturation and evidence for the role of a Galpha during uptake. *Cell Microbiol* **5:** 2228–2243

Grode, L., Seiler, P., Baumann, S., Hess, J., Brinkmann, V., Nasser Eddine, A., *et al.* (2005) Increased vaccine efficacy against tuberculosis of recombinant *Mycobacterium bovis* bacille Calmette–Guerin mutants that secrete listeriolysin. *J Clin Invest* **115:** 2472–2479.

Hagedorn, M., Neuhaus, E.M., and Soldati, T. (2006) Optimised fixation and immunofluorescence staining methods for *Dictyostelium* cells. *Methods Mol Biol* **346:** 327–338.

Hagele, S., Kohler, R., Merkert, H., Schleicher, M., Hacker, J., and Steinert, M. (2000) Dictyostelium discoideum: a new host model system for intracellular pathogens of the genus Legionella. *Cell Microbiol* **2:** 165–171.

Hiller, N.L., Akompong, T., Morrow, J.S., Holder, A.A., and Haldar, K. (2003) Identification of a stomatin orthologue in vacuoles induced in human erythrocytes by malaria parasites. A role for microbial raft proteins in apicomplexan vacuole biogenesis. *J Biol Chem* **278:** 48413–48421.

Jenne, N., Rauchenberger, R., Hacker, U., Kast, T., and Maniak, M. (1998) Targeted gene disruption reveals a role for vacuolin B in the late endocytic pathway and exocytosis. *J Cell Sci* **111:** 61–70.

Journet, A., Chapel, A., Jehan, S., Adessi, C., Freeze, H., Klein, G., and Garin, J. (1999) Characterization of *Dictyostelium discoideum* cathepsin D. Molecular cloning, gene disruption, endo-lysosomal localization and sugar modifications. *J Cell Sci* **112:** 3833–3843.

Kobayashi, T., Stang, E., Fang, K.S., de Moerloose, P., Parton, R.G., and Gruenberg, J. (1998) A lipid associated with the antiphospholipid syndrome regulates endosome structure and function. *Nature* **392:** 193–197.

Maniak, M. (2002) Conserved features of endocytosis in *Dictyostelium*. *Int Rev Cytol* **221:** 257–287.

Maniak, M. (2003) Fusion and fission events in the endocytic pathway of *Dictyostelium*. *Traffic* **4:** 1–5.

McDonough, K.A., Kress, Y., and Bloom, B.R. (1993) Pathogenesis of tuberculosis: interaction of *Mycobacterium tuberculosis* with macrophages. *Infect Immun* **61:** 2763–2773.

Neuhaus, E.M., Horstmann, H., Almers, W., Maniak, M., and Soldati, T. (1998) Ethane-freezing/methanol-fixation of cell monolayers. A procedure for improved preservation of structure and antigenicity for light and electron microscopies. *J Struct Biol* **121:** 326–342.

Neuhaus, E.M., Almers, W., and Soldati, T. (2002) Morphology and dynamics of the endocytic pathway in *Dictyostelium discoideum*. *Mol Biol Cell* **13:** 1390–1407.

Nose, Y., Rees, E.M., and Thiele, D.J. (2006) Structure of the Ctr1 copper trans'PORE'ter reveals novel architecture. *Trends Biochem Sci* **31:** 604–607.

Peracino, B., Wagner, C., Balest, A., Balbo, A., Pergolizzi, B., Noegel, A.A., *et al.* (2006) Function and mechanism of action of *Dictyostelium* Nramp1 (Slc11a1) in bacterial infection. *Traffic* **7:** 22–38.

Philips, J.A., Rubin, E.J., and Perrimon, N. (2005) Drosophila RNAi screen reveals CD36 family member required for mycobacterial infection. *Science* **309:** 1251–1253.

Piddington, D.L., Fang, F.C., Laessig, T., Cooper, A.M., Orme, I.M., and Buchmeier, N.A. (2001) Cu,Zn superoxide dismutase of *Mycobacterium tuberculosis* contributes to survival in activated macrophages that are generating an oxidative burst. *Infect Immun* **69:** 4980–4987.

van Pittius, N.C.G., Sampson, L.S., Lee, H., Kim, Y., van Helden, P.D., and Warren, R.M. (2006) Evolution and expansion of the *Mycobacterium tuberculosis* PE and PPE multigene families and their association with the duplication of the ESAT-6 (*esx*) gene cluster regions. *BMC Evol Biol* **6:** 1471–2148.

Pozos, T.C., and Ramakrishnan, L. (2004) New models for the study of *Mycobacterium*–host interactions. *Curr Opin Immunol* **16:** 499–505.

Pukatzki, S., Kessin, R.H., and Mekalanos, J.J. (2002) The human pathogen *Pseudomonas aeruginosa* utilizes conserved virulence pathways to infect the social amoeba *Dictyostelium discoideum*. *Proc Natl Acad Sci USA* **99:** 3159–3164.

Pukatzki, S., Ma, A.T., Sturtevant, D., Krastins, B., Sarracino, D., Nelson, W.C., *et al.* (2006) Identification of a conserved bacterial protein secretion system in *Vibrio cholerae* using the *Dictyostelium* host model system. *Proc Natl Acad Sci USA* **103:** 1528–1533.

Ramakrishnan, L., Federspiel, N.A., and Falkow, S. (2000) Granuloma-specific expression of *Mycobacterium virulence* proteins from the glycine-rich PE-PGRS family. *Science* **288:** 1436–1439.

Rauchenberger, R., Hacker, U., Murphy, J., Niewohner, J., and Maniak, M. (1997) Coronin and vacuolin identify consecutive stages of a late, actin-coated endocytic compartment in *Dictyostelium*. *Curr Biol* **7:** 215–218.

Ravanel, K., de Chassey, B., Cornillon, S., Benghezal, M., Zulianello, L., Gebbie, L., *et al.* (2001) Membrane sorting in the endocytic and phagocytic pathway of *Dictyostelium discoideum*. *Eur J Cell Biol* **80:** 754–764.

Russell, D.G. (2001) *Mycobacterium tuberculosis*: here today, and here tomorrow. *Nat Rev Mol Cell Biol* **2:** 569–577.

Schuller, S., Neefjes, J., Ottenhoff, T., Thole, J., and Young, D. (2001) Coronin is involved in uptake of *Mycobacterium bovis* BCG in human macrophages but not in phagosome maintenance. *Cell Microbiol* **3:** 785–793.

Solomon, J.M., Rupper, A., Cardelli, J.A., and Isberg, R.R. (2000) Intracellular growth of *Legionella pneumophila* in *Dictyostelium discoideum*, a system for genetic analysis of host–pathogen interactions. *Infect Immun* **68:** 2939–2947.

Solomon, J.M., Leung, G.S., and Isberg, R.R. (2003) Intracellular replication of *Mycobacterium marinum* within *Dictyostelium discoideum*: efficient replication in the absence of host coronin. *Infect Immun* **71:** 3578–3586.

Somesh, B.P., Neffgen, C., Iijima, M., Devreotes, P., and Rivero, F. (2006) *Dictyostelium* RacH regulates endocytic vesicular trafficking and is required for localization of vacuolin. *Traffic* **7:** 1194–1212.

Stamm, L.M., Morisaki, J.H., Gao, L.Y., Jeng, R.L., McDonald, K.L., Roth, R., *et al.* (2003) *Mycobacterium marinum* escapes from phagosomes and is propelled by actin-based motility. *J Exp Med* **198:** 1361–1368.

Stamm, L.M., Pak, M.A., Morisaki, J.H., Snapper, S.B., Rottner, K., Lommel, S., and Brown, E.J. (2005) Role of the WASP family proteins for *Mycobacterium marinum* actin tail formation. *Proc Natl Acad Sci USA* **102:** 14837–14842.

Sturgill-Koszycki, S., Schlesinger, P.H., Chakraborty, P., Haddix, P.L., Collins, H.L., Fok, A.K., *et al.* (1994) Lack of acidification in *Mycobacterium* phagosomes produced by exclusion of the vesicular proton-ATPase. *Science* **263:** 678–681.

Sturgill-Koszycki, S., Schaible, U.E., and Russell, D.G. (1996) *Mycobacterium*-containing phagosomes are accessible to early endosomes and reflect a transitional state in normal phagosome biogenesis. *EMBO J* **15:** 6960–6968.

Swaim, L.E., Connolly, L.E., Volkman, H.E., Humbert, O., Born, D.E., and Ramakrishnan, L. (2006) *Mycobacterium marinum* infection of adult zebrafish causes caseating granulomatous tuberculosis and is moderated by adaptive immunity. *Infect Immun* **74:** 6108–6117.

Tan, T., Lee, W.L., Alexander, D.C., Grinstein, S., and Liu, J. (2006) The ESAT-6/CFP-10 secretion system of *Mycobacterium marinum* modulates phagosome maturation. *Cell Microbiol* **8:** 1417–1429.

Vergne, I., Chua, J., Singh, S.B., and Deretic, V. (2004a) Cell biology of mycobacterium tuberculosis phagosome. *Annu Rev Cell Dev Biol* **20:** 367–394.

Vergne, I., Fratti, R.A., Hill, P.J., Chua, J., Belisle, J., and Deretic, V. (2004b) *Mycobacterium tuberculosis* phagosome maturation arrest: mycobacterial phosphatidylinositol analog phosphatidylinositol mannoside stimulates early endosomal fusion. *Mol Biol Cell* **15:** 751–760.

Vergne, I., Singh, S., Roberts, E., Kyei, G., Master, S., Harris, J., *et al.* (2006) Autophagy in immune defense against mycobacterium tuberculosis. *Autophagy* **2:** 175–178.

Volkman, H.E., Clay, H., Beery, D., Chang, J.C., Sherman, D.R., and Ramakrishnan, L. (2004) Tuberculous granuloma formation is enhanced by a mycobacterium virulence determinant. *PLoS Biol* **2:** e367.

Weber, S.S., Ragaz, C., Reus, K., Nyfeler, Y., and Hilbi, H. (2006) *Legionella pneumophila* exploits PI(4)P to anchor secreted effector proteins to the replicative vacuole. *PLoS Pathog* **2:** e46.

van der Wel, N., Hava, D., Houben, D., Fluitsma, D., van Zon, M., Brenner, M., and Peters, P. (2007) *M. tuberculosis* and *M. leprae* translocate from the phagolysosome to the cytosol in myeloid cells. *Cell* (in press).

Wienke, D., Drengk, A., Schmauch, C., Jenne, N., and Maniak, M. (2006) Vacuolin, a flotillin/reggie-related protein from *Dictyostelium* oligomerizes for endosome association. *Eur J Cell Biol* **85:** 991–1000.

Supplementary material

The following supplementary material is available for this article online:

Fig. S1. Quantitative analysis of the infection p. Adherent *Dictyostelium* cells were synchronously infected with GFP-expressing wild type *M. marinum* (mar wt), avirulent *M. marinum* L1D (mar L1D) and non-pathogenic *M. smegmatis* (smeg) by centrifuging the mycobacteria onto the cells. At 0.5 hpi, uningested mycobacteria were removed and cells were further incubated in shaking conditions. (a) At the indicated times, samples of the infected cultures were briefly centrifuged onto coverslips, fixed and the proportion of infected cells (bar graph ± SEM) and the number of bacteria per cell (scatter plot) were scored by direct visualisation with a fluorescence microscope. (b) Samples of the infected cultures at 0.5 and 1.5 hpi were also analysed by FACS, by plotting side scattering (SSC) as a function of fluorescence (FL1). At 0.5 hpi, the proportion of cells containing fluorescent mycobacteria was very similar for all three strains, but one hour later the fate of the infected cell population was markedly different (delimited by a black box at 1.5 hpi). Whereas *M. marinum* L1D was almost completely exocytosed from the host cells at 1.5 hpi, wild type *M. marinum* and *M. smegmatis* were mainly present within the host cells.

Fig. S2. Phagosomes containing *M. marinum* divert from the normal maturation programme in *Dictyostelium*. Uptake of the three mycobacteria strains was performed as in Fig. S1 and the fate of cells containing fluorescent mycobacteria was monitored every 3 h during phase 1 of infection by immunofluorescent staining and microscopy of three phagosome maturation markers: the VatA subunit of the vacuolar H^+-ATPase (a marker of early maturation), the lysosomal hydrolase cathepsin D (CatD; a marker of intermediate maturation), and the flotillin homologue vacuolin (Vac; a marker of the late re-neutralized phagolysosomal compartment prepared for exocytosis of undigested remnants). Representative images of colocalisation at 6 hpi are shown for (a) VatA and CatD and (b) Vac and CatD. Arrows indicate fluorescent wild type *M. marinum* that did not colocalize with the maturation markers. Arrowheads point to mycobacteria that colocalized with one (white arrowheads) or both of the markers (black arrowheads).

Fig. S3. Infection of *racH*$^-$ cells with *M. marinum* L1D. Adherent *Dictyostelium* cells lacking RacH (*racH*$^-$ cells) were synchronously infected with GFP-expressing *M. marinum* L1D (mar L1D) by centrifuging the mycobacteria onto the cells. After removal of uningested mycobacteria at 0.5 hpi, the cells were incubated until 43 hpi. At the indicated times, samples from the infection were taken and analysed by FACS. (a) Plotting side scattering (SSC) as a function of fluorescence (FL1) revealed differences in the course of infection. (b) The total fluorescent signal in the infected culture (infected cells and extracellular bacteria) was integrated at each time point (shown for 0.5 hpi in the left panel) and normalised to allow direct comparison of the time profiles (right panel). (c) The number of live bacteria was determined by counting CFUs at the indicated times (shown for 0.5 hpi, left panel) and also normalised to allow direct comparion of the time profiles (right panel). (d) Representative examples of *racH*$^-$ cells infected with *M. marinum* L1D at 21 hpi, stained for VatA and vacuolin. Arrowheads and arrows indicate bacteria positive and negative, respectively, for each marker. Scale bar 5 μm.

This material is available as part of the online article from:
http://www.blackwell-synergy.com/doi/abs/10.1111/j.1462-5822.2007.00993.x

Please note: Blackwell Publishing is not responsible for the content or functionality of any supplementary materials supplied by the authors. Any queries (other than missing material) should be directed to the corresponding author for the article.

